Tailored porosities of the cathode layer for improved polymer electrolyte fuel cell performance

A. Zlotorowicz [a], K. Jayasayee [b], P.I. Dahl [b], M.S. Thomassen [b], S. Kjelstrup [a,*]

[a] Department of Chemistry, Norwegian University of Science and Technology, NO-7491 Trondheim, Norway
[b] SINTEF Materials and Chemistry, NO-7465 Trondheim, Norway

HIGHLIGHTS

- A new technique, that introduces micrometer sized pores in the nanoporous catalyst layer, is tested.
- The technique uses monodisperse polystyrene particles as pore formers.
- Macropores in the nanoporous layer improves the polymer electrolyte fuel cell performance.
- Results are obtained for catalyst loading which are twice the US DOE target for 2020.

GRAPHICAL ABSTRACT
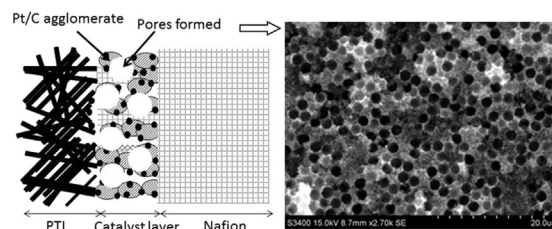
ABSTRACT

We show experimentally for the first time that the introduction of macro-pores in the nanoporous catalyst layer of a polymer electrolyte membrane fuel cell can improve its performance. We have achieved a Pt utilization of about 0.23 mg W^{-1} at 0.6 V which is twice the value of the DOE target for 2020, and three times (0.60 mg W^{-1}) smaller than the value of a fully nanoporous reference layer at a catalyst loading of 0.11 mg cm^{-2}. In this work, monodispersed polystyrene particles with diameters of 0.5 and 1 μm were used as pore formers. Cathode catalyst layers with macroporous volume fractions between 0 and 0.58 were investigated. Maximum performance was observed for fuel cells with a macroporous volume fraction of about 0.52 for a 1 μm thick catalyst layer. The results, which were obtained for the cathode layer, support earlier theoretical predictions that gas access to and water escape from the catalyst can be facilitated by introduction of macropores in the nanoporous layer.

1. Introduction

The use of the polymer electrolyte membrane fuel cell (PEMFC) for transport applications requires electrodes that produce a high power density with low catalyst loading. The US-DOE has set the target of reducing the PGM (Pt group metal) content to about 0.125 mg W^{-1} for automotive use in the year 2020 [1]. This implies that PEMFCs must be able to operate at high current densities with an acceptable reduction in cell potential and low material costs. High current densities mean significant ohmic losses in the membrane and high cathode overpotentials. Operations at high current densities lead to insufficient oxygen supply to the cathode. Water clogging of the pores can also hamper oxygen access. This will create oxygen concentration gradients across the catalyst layer resulting in decreased fuel cell performance.

* Corresponding author.
E-mail address: signe.kjelstrup@ntnu.no (S. Kjelstrup).

The first significantly improved PEMFC performance was achieved when the thin film MEA catalyst layer with low platinum loading (~0.1 mg cm^{-2}) was introduced in 1992 [2,3]. Since then, different methods that improve the performance and reduce the Pt utilization further, have been reported [4–26]. Attention has been given to modifications of pore structure, *e.g.* by using different catalyst supported carbons [4,5], to variations in the carbon composition [6], to varying Nafion content [7–10] and to pore formers of various sorts [11–15]. The importance of the morphological properties of the gas/water supply pathway on the performance has been studied extensively; see *e.g.* Refs. [16–19]. The morphology of the catalyst layer, however, has only recently been addressed [20–26]. The relation between the pore size, morphology, distribution and synthesis, and the cell performance is therefore not fully understood.

Kjelstrup et al. [20] proposed a systematic route to MEA design. Using the experience that minimum energy dissipation can be obtained with uniform driving forces [21,22], a strategy was proposed to minimize concentration polarization in the PEMFC. The strategy was inspired by theoretical work of Wang and Coppens [24] for effective heterogeneous catalysis. It was predicted that better performance with lower Pt utilization was achievable by the introduction of optimal macropores in the catalyst layer [20]. This would facilitate a more uniform and rapid distribution of oxygen and product water than in a fully nanoporous layer. There is not yet such general procedure adopted in the production of MEAs, and the present work, along with our recent publication [14], can be seen as first steps in this direction. We have chosen to investigate the effect on the cathode where the potential for improvements are largest.

In their theoretical optimization procedure, Kjelstrup et al. [20] found the optimal macroporosity and the height of the catalyst layer in the polymer electrolyte fuel cell. As a calculation example, they used the standard E-TEK Elat/Std/DS/V2 gas diffusion electrodes with 0.5 mg of Pt cm^{-2} catalyst loading, and 20% Pt/C on Vulcan XC-72 as a catalyst support. It was found that the amount of catalyst could possibly be reduced by a factor of 4–8, while the energy efficiency for the same conditions (high current density) could be increased by 10–20%. It was further shown that an optimal macroporosity existed when the pore volume fraction was 0.5. The optimum was shallow (see Fig. 3 in Ref. [20]), meaning that a variation in 0.5 by ±0.2 units did not make much of a difference for the outcome of the calculation. The upper bound of the pore diameter was 0.5 μm. The value obtained for the thickness of the catalyst layer (4 μm for a current density of 1.5 A cm^{-2}) depended on assumptions of (i) a first-order reaction at the cathode, (ii) the value of the gas diffusion constant for oxygen (iii) the oxygen concentration in the inlet flow.

It is not trivial to create catalyst layers which have a uniformly distributed macroporosity. To use indentation techniques, templates etc. is close at hand [11,12,14], but these procedures are costly and cumbersome at their present stage of development. We ourselves were struggling to fabricate catalyst layers with pores <2 μm through template-assisted indentation methods [14]). The theoretical results mentioned above are useful in this situation, as they make clear that the exact value of the macroporosity, as well as the pore shape is not essential for achieving improvements. To us, this means that it is not necessary to implement straight and well defined channel-like macropores into the nanoporous catalyst layer.

For this reason, we have turned our attention to the possibility offered by polystyrene monodisperse particles [14]. The fact that they are monodisperse means that we can determine the volume fraction of macropores that they can introduce in the catalyst layer. In this work, we have chosen to work with particles of diameter 1 and also 0.5 μm. We have not been able to go below the smallest

diameter yet, and a larger diameter will disturb the charge-conducting pathways too much. The values chosen can be seen as approximations to the optimal theoretical value of 0.5 μm [20]. We shall see that the fuel cell with 0.5 μm pores perform better than the one with larger pores.

The idea of the procedure is schematically pictured in Fig. 1. The figure shows the half-cell that contains the cathode before (a) and after (b) the introduction of macropores. The reference cell (a) has a fully nanoporous catalyst layer with Pt/C particles in contact with the Nafion 212 membrane on one side and a porous transport layer (PTL) or the current collector on the other side. Test cell (b) shows homogeneous macropores created by introduction of polystyrene particles in the nanoporous catalyst layer. The membrane and PTL are the same in Fig. 1b and a. In Fig. 1a, the reacting gas is supplied to the catalyst particles through nanopores only, while in Fig. 1b, the reacting gas can travel in two types of pores, one large with diameter 0.5 or 1.0 μm, and one small with a nanometer diameter. The large pores serve as a short-cut path for the gas to the catalyst, and a better escape possibility for water in the reverse direction. The total layer thickness in the Figure is 1 μm, meaning that there is space for maximum one sphere of diameter 1 μm, but two layers of particles having a diameter 0.5 μm. The last case is illustrated in Fig. 1b.

We show first how the monodisperse particles can be added to the synthesis mixture and removed before the MEA is made. The resulting layer, with macropores embedded in a nanoporous mixture, is tested under normal fuel cell conditions. We shall see that the results agree with the theoretical predictions [20]. Micro-spherical cavities with 0.5 μm diameter, packed to a volume fraction 0.52 in a layer of thickness 1 μm, improve the catalyst utilization (mg W^{-1}) by a factor of three compared to a reference layer without macropores. Although the performance of fuel cell with larger macropores is comparatively inferior it is still better than the reference cell without any macropores.

We explain in Section 2 how the novel catalyst layers with pore formers were made and tested for fuel cell performance. Scanning electron micrographs (SEM) were taken to ensure that we created a homogeneous porosity. The results from the first tests of the effect of monodisperse pore formers, described in Section 3.2, confirm the theoretical predictions made, which leads us to conclude in Section 4 that this line of research should be pursued.

2. Experimental

2.1. Preparation of membrane electrode assembly

The schematic preparation process of a paste for the catalyst layers was described in our previous publication [14]. A conventional anode was used, to be able to conclude on the cathode performance directly. Porous transport layers (PTLs) of type H2315 I2 C6 from Freudenberg (FCCT), to be used as anodes, were manually sprayed with 40 wt% Pt/C to give a loading of about 0.4 mg cm^{-2}. In the reference experiments we used this layer also at the cathode.

Monodispersed polystyrene particles were introduced as pore formers in the cathode catalyst layer only. The polystyrene particles with the diameters of 0.5 and 1.0 μm were synthesized in-house by the Division of Polymer and Composite Materials at SINTEF Materials and Chemistry. The amount of polystyrene particles to be tested was dispersed in water and added to the catalyst ink. The ink was prepared by mixing 60 wt% Pt/C (Alfa Aesar GmbH&CoKG) with isopropanol and deionized water (ratio 4:1) with 17 wt% Nafion solution (DuPont Inc.) with respect to Pt/C, and polystyrene particles with wt% 0, 30, 50, 70 or 90 with respect to Pt/C. The Pt loading in the dry cathode catalyst layer was fixed between 0.10 and 0.12 mg cm^{-2}. This serves as our reference catalyst for
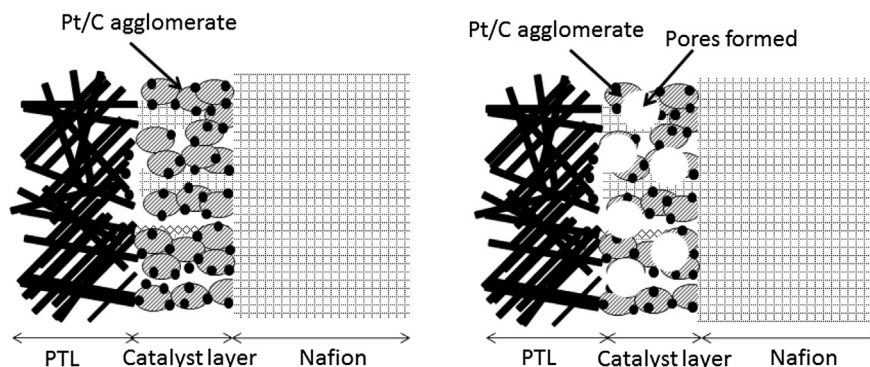
Fig. 1. Schematic cross section of half the MEA without the micrometer pores formed (left) and with such pores formed in the cathode part (right). Only one electrode (the cathode) is shown. The amount of nanoporous material in the catalyst layer (or the Pt/C catalyst) will vary with the diameter and the amount of pore former.

performance comparisons. The catalyst ink with polystyrene particles was manually sprayed on Nafion 212 membrane (Ion Power, Inc.) using an air brush until a layer thickness of 1 μm was produced. The layer was next dried at 80 °C for 30 min. The resulting catalyst coated membrane (CCM) was then immersed in a container containing ethyl acetate (Sigma—Aldrich) at room temperature for about 2 h in order to remove polystyrene particles from the catalyst layer and obtain the wanted pores. It was found through scanning electron micrographs (SEM) that 2 h were sufficient to dissolve all polystyrene beads from the catalyst layer. The CCM was then washed in boiling water a few times to make sure that the final CCM was free of ethyl acetate.

MEAs with an area of 5 cm^2, were fabricated by sandwiching the freshly made CCM between PTLs. In the final configuration only the catalyst layer contained monodisperse holes. The flow field plate of the anode had a single serpentine pattern while the cathode had a double serpentine flow field design. The fuel cell assembly was compressed with a torque of 5 Nm on 8 bolts.

The Pt loading of the reference layer was first determined by direct weighing to be 0.11 ± 0.01 mg cm^{-2}. The weight ratios were also used to calculate the loading as well as the volume fractions of PS. The densities of graphite (C) [27], platinum [28], Nafion [29] and polystyrene (PS) [30] were (in g cm^{-3}) 2.27, 21.45, 1.64 and 1.05, respectively. The mass of each component was given relative to carbon giving m_C:m_{Pt}:m_{Nafion}:m_{PS} = 100:60:17: x where x is the wt% of PS. This was introduced in the relation $\sum_i (m_i/\rho_i) = V$ for i = C, Pt, Nafion, PS, with the layer volume $V = 5 \times 10^{-6}$ cm^3. From this we calculated the Pt loading in the various samples to 0.040, 0.047, 0.054, 0.065 and 0.11 mg cm^{-2}. The results are given in Table 1. The accuracy in these numbers is estimated to 10%.

The value for the reference membrane ($x = 0$) agreed with the

result obtained from weighing of Pt before applying it, 0.11 mg cm^{-2}. The average loading in the reference case from both methods of determination was then 0.11 ± 0.1 mg cm^{-2}. The formula was next used to convert the weight per cents (0, 30, 50, 70, 90) into the corresponding volume fraction, see Table 1 for results.

2.1.1. SEM analysis

A Hitachi S-3400N scanning electron microscope (SEM) was used for the SEM investigations. A working distance of 15 mm with an acceleration voltage of 20 kV was used. The instrument was operated in the high vacuum mode. Several images were taken of the same batch. Pictures are shown for a typical preparation.

2.1.2. Fuel cell testing

Fuel cell tests were carried out at 60 °C with hydrogen and air at 1 bar as fuel and oxidant. The relative humidity of the anode was kept fixed at 80% throughout the measurements while the cathode humidity was 100%. The stoichiometric ratio of hydrogen to oxygen was maintained at 2.0 throughout the testing. The MEAs were conditioned by a pulsating potential, varying between 0.7 and 0.3 V for 24 h before the polarization curve was recorded. The measurements were repeated successfully twice with the same batch of fresh materials.

3. Results and discussion

We report first on the outcome of the catalyst layer synthesis procedure described above. We shall see that the procedure produces a nanoporous layer in the cathode containing micrometer-sized pores. The original layer has in contrast, nanometer-sized pores only. The original and new cathode catalyst layers are tested in a fuel cell. The cell with the new cathode layer were shown to perform better than a cell with a nanoporous catalyst cathode layer. Perspectives on these results are given in the end of the section.

3.1. Surface characterization

Fig. 2 shows a SEM image of polystyrene particles dispersed in water. The polystyrene particles are spherical-shaped and we can find that the diameter is about 0.5 μm. No agglomerates were observed, and the particles were well distributed.

Fig. 3 shows a SEM micrograph of the morphology of the nanoporous catalyst layers with 20 wt% of 1 μm diameter polystyrene particles with respect to Pt/C loading embedded. On the surface we observe visible and homogeneously distributed beads which correspond to the polystyrene particles before dissolution in

Table 1
Cathode layer characteristics and results from evaluation of fuel cell polarization curves at 0.4 and 0.6 V.

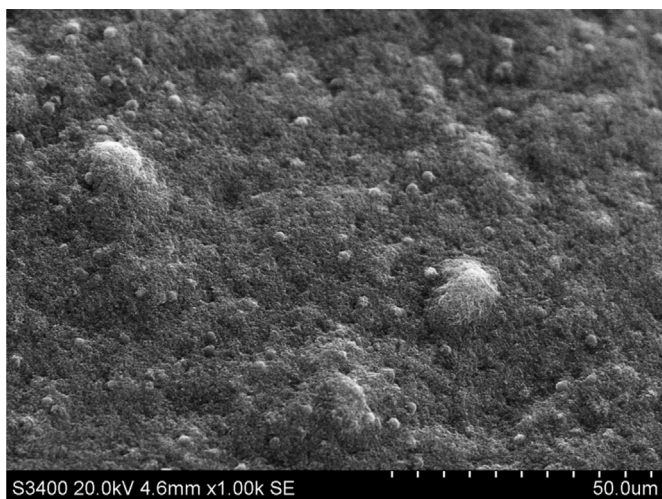| PS wt%, d/μm	PS vol%	Pt loading mg cm^{-2}	PD W cm^{-2} (0.4 V)	mg/W (0.4 V)	PD W cm^{-2} (0.6 V)	mg/W (0.6 V)
0	0	0.11	0.22	0.50	0.15	0.74
30 (1)	31	0.065	0.18		0.15	
50 (1)	43	0.054	0.18		0.13	
70 (1)	52	0.047	0.25	0.19	0.16	0.29
90 (1)	58	0.040	0.20		0.15	
70 (0.5)	52	0.047	0.30	0.16	0.20	0.23

Layer volume was 5×10^{-4} cm^3. Densities were taken from the literature [27–30]. PS: polystyrene C: graphite Pt: platinum PD: power density.
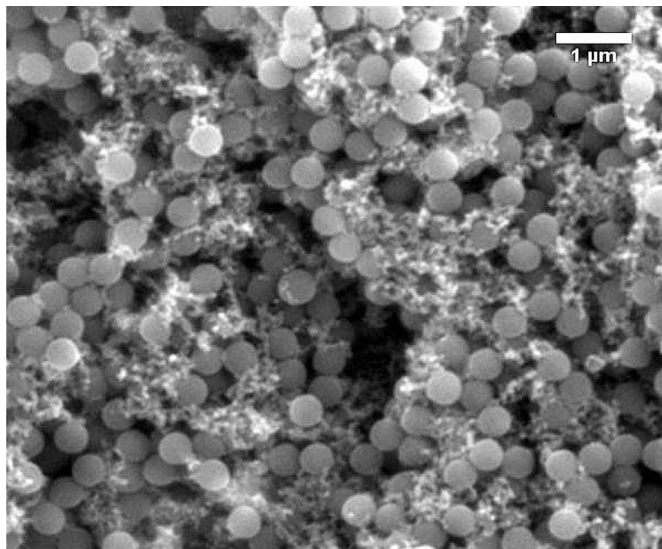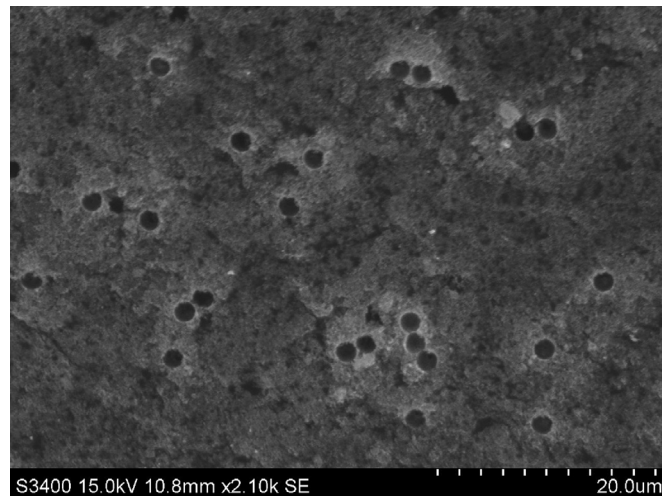
Fig. 2. SEM image of the polystyrene particles 0.5 μm to be used as pore former, dispersed in water.

Fig. 4. Catalyst layer with pores formed by the removal of 40 wt% of 1 μm monodispersed polystyrene particles. The layer has a mixture of nano- and micrometer sized pores.
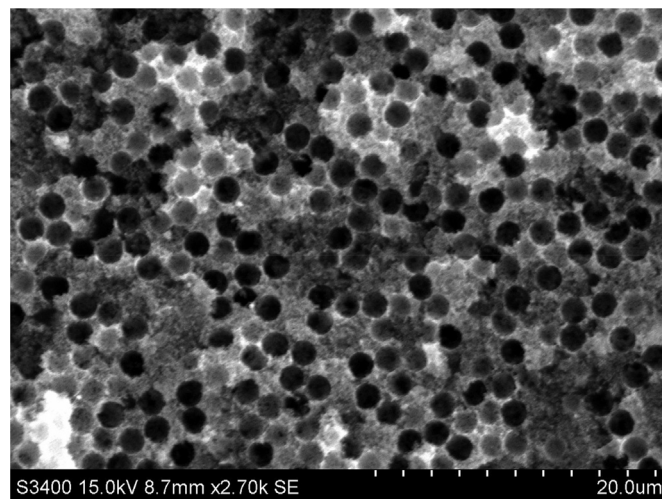
ethyl acetate.

Figs. 4 and 5 show the SEM image of the catalyst layer with pores formed by the removal 40 and 70 wt% of 1 μm monodisperse polystyrene particles, *cf.* Table 1, respectively. The pores formed through the dissolution of these particles are clearly spherical-shaped. The images show that the density of pores increases with an increase in polystyrene loading in the catalyst layer. The pore shape, size and distribution are found to be homogenous without any agglomeration, even in the case of the high loading, 70 wt% polystyrene. Also, the insertion and removal procedure reproduces the original diameter of the polystyrene particles, suggesting that the original particles did not swell before or during electrode preparation. This means that polystyrene particles can be used successfully to introduce well-defined and homogeneously distributed pores in a layer. This makes this procedure beneficial compared to other preparation procedures. Template techniques for introduction of macropores are more cumbersome and/or expensive [14].

Fig. 5. Catalyst layer with micro-pores added by removal of 70 wt% of 1 μm monodispersed polystyrene particles.

The pictures presented in Figs. 4 and 5 allow us also to estimate the volume fraction occupied by the spheres. Assuming that there is only one layer of spheres in the catalyst layer, we can calculate this fraction from the average number of spheres in an area, the single sphere volume and the volume of the total layer. The average number of particles was found from analysis of five images to be 20 ± 2 in a volume of 1×10^{-10} cm^{-3}. The results of this calculation for spheres of 1 μm with 70 wt% PS added gave a volume fraction of $80 \pm 10\%$, which is much higher than the fraction given in Table 1. If the same calculation is done for spheres of a smaller diameter, the volume fraction drops to 20%. The averaging procedure used may not be sufficient for good statistics. In lack of an explanation for this, we continue with the results in Table 1.

Altogether, this means that we have successfully synthesized a catalyst layer where one or two monodisperse spheres can provide a high conductivity path for reactants and products. Thanks to this path, they will be able to travel essentially in the gas phase almost up to the site where the electrochemical reaction can take place. We shall see that the test of such a layer in a fuel cell test station, indeed confirms that this is favorable for the performance.

Fig. 3. Nanoporous catalyst layer with monodispersed polystyrene particles having a diameter of 1 μm.

3.2. Fuel cell – single cell tests

The MEAs prepared in-house with different amounts (0, 30, 50, 70 and 90 wt%) of polystyrene pore formers in the catalyst layers were tested under the operating conditions described above. The MEA without polystyrene pore former (0 wt%) was used as reference. This reference has a Pt loading of 0.11 mg cm^{-2} (cf. Table 1).

Fig. 6 shows polarization curves for pore formers of 1 μm. The figure compares the effect of polystyrene loading on the fuel cell performance at 80/100% anode/cathode relative humidity and 2.0/2.0 hydrogen and air stoichiometry. Neither of the curves show any change in curvature at high current densities (small mass transfer limitations). We see for these conditions that the performance of the fuel cell, in terms of its current–voltage relationship (or polarization curve) is best for 70 wt% polystyrene.

The variation due to introduction of macropores, documented in Fig. 6, allow us to conclude that a mixture of nano- and micropores in the catalyst layer could aid water and gas transport in the cathode. To quantify the performance, we calculated the power density for 0 and 70 wt% PS at 0.4 V. The result was 0.22 and 0.25 W cm^{-2}, giving also 0.50 and 0.19 mg W^{-1}. The results of calculations are given in Table 1.

It is interesting that there is an optimum in the wt% of polystyrene; a value which performs better than other loadings. Within the range of compositions investigated here the optimum is near 70 wt% or 52 vol%. The true optimum can most probably be found by more experiments, considering that the optimum line is closer to the 90 wt% line, than to the 50 wt% line. An optimum at a higher wt% means higher savings of Pt. At this stage, we note that an optimum in the curve has been found, in agreement with the theoretical predictions [19].

Fig. 7 compares the effect of spheres with diameters 1 and 0.5 μm, on the fuel cell polarization curves at 80/100% anode/cathode relative humidity and 2.0/2.0 hydrogen and air stoichiometry. The performance is better when the sphere diameter is 0.5 μm compared to 1 μm. In terms of power density we obtain 0.30 W cm^{-2} at 0.4 V, compared to the reference value of 0.22 W cm^{-2} and a value for larger pores, 0.25 W cm^{-2}, reported

Fig. 7. Polarization curve comparing the performance of a reference MEA (0 wt% PS) with a MEA with micrometer sized pore formers (0.5 and 1 μm spheres) of various wt%. All experiments were done at 100% cathode relative humidity and 2.0/2.0 H$_2$/air stoichiometry.

above. Table 1 gives a summary of the essential values.

Clearly, there is a trade-off between micropore- and nanopore volumes. This is also expected from the calculations [20], and should be further investigated. It is remarkable that the results confirm the original calculation, not only in a qualitative manner, but also in a quantitative way. It was predicted that an optimal pore size should be near 0.5 μm, given certain conditions like the diffusion coefficient of oxygen in the gas phase. A sphere diameter is of course not the same as the diameter of a straight channel. The variation in pore shape in the direction of transport must be taken into account. Nevertheless we obtain meaningful enhancements in for a reasonable sphere size.

The findings of Saha et al. [23] may be seen as giving experimental support to the main idea. They used a colloidal monomer containing ink in their preparation of the catalyst layer, and found an enhanced performance of the polymer electrolyte fuel cell, which possibly could be associated with an introduction of larger pores. The optimization results of Marquis and Coppens [25] can be seen as theoretical support. They showed that ultralow platinum loadings were possible by an agglomerate model of the catalyst layer. It will now be important to investigate experimentally the effect of monodisperse particle pore formers at a varying platinum loading.

We have shown that the introduction of macropores in the nanoporous catalyst layer can increase the yield of the catalyst by a factor 3, and that we are only a factor of 2 higher than the DOE target for 2020. There are several important additional subjects for possible further optimizations, for instance the Nafion content, the catalyst layer thickness and the Pt loading etc. It will be important to study by experiments the role of water in the new layer, as water transport is known to be decisive for good cathode performance. It will not be surprising if the combination of nano- and micropores turns out to be beneficial also for water removal [20].

4. Conclusion

A new catalyst layer preparation technique was successfully carried out and tested in a polymer electrolyte fuel cell. The idea to introduce macropores into the nanoporous catalyst layer was realized through introduction of monodisperse polystyrene
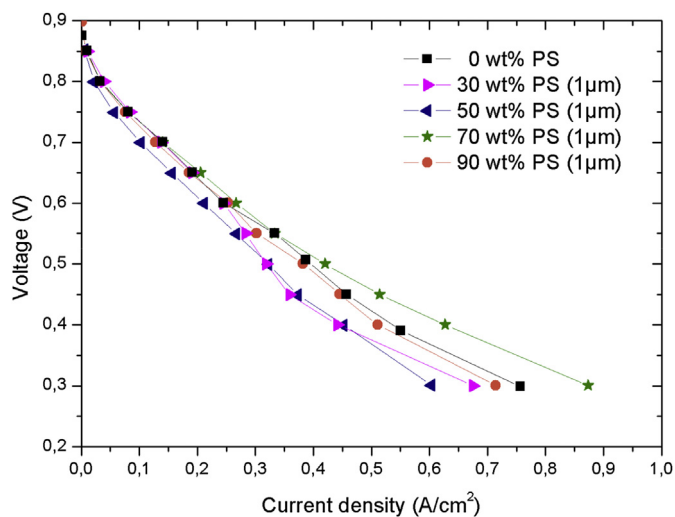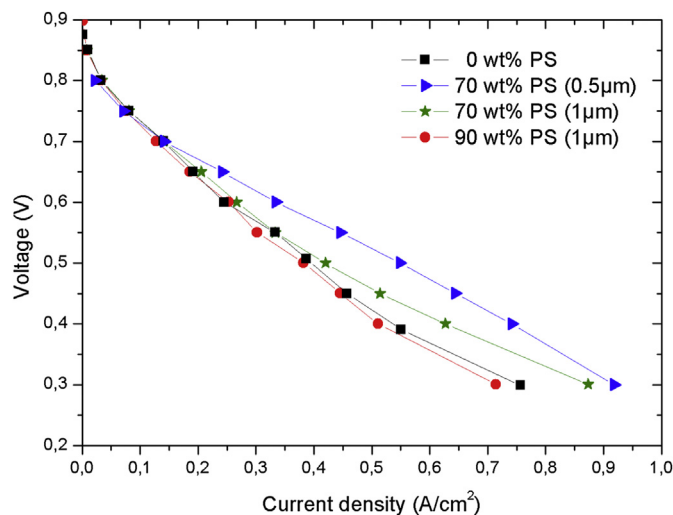
Fig. 6. Polarization curve comparing the performance of normal MEA and a MEA with micro and nanopores, at 100% cathode RH and 2.0/2.0 H$_2$/air stoichiometry All polystyrene (PS) particles used as pore formers were 1 μm. Results are shown for 0, 30, 50, 70 and 90 wt% PS, where 0 means a fully nanoporous layer (the reference).

particles in the MEA synthesis step, and by removal of these particles in a later stage. A significant performance increase was seen by the introduction of micrometer sized pores giving a volume fraction of 0.52. Their introduction in the nanoporous catalyst layer reduced the amount of Pt needed for power production by a factor three compared to fully nanoporous layer. The value obtained is twice the DOE target for 2020. The design of a catalyst layer was predicted by a mathematical optimization procedure considering the main transport processes in the layer, meaning that we can take advantage of a systematic procedure. Further optimizations can be done.

Acknowledgments

References

[1] See pages 26-28 in the report: http://energy.gov/sites/prod/files/2014/03/f12/fuel_cells.pdf
[2] M.S. Wilson, S. Gottesfeld, J. Electrochem. Soc. 139 (1992) 28.
[3] M.S. Wilson, S. Gottesfeld, J. Appl. Electrochem. 22 (1) (1992) L1.
[4] N. Jia, R.B. Martin, Z. Qi, M.C. Lefebvre, P.G. Pickup, Electrochim. Acta 46 (2001) 2863.
[5] X. Wang, I.M. Hsing, P.L. Yue, J. Power Sources 96 (2001) 282.
[6] T. Soboleva, X. Zhao, K. Malek, Z. Xie, S. Holdcroft, Appl. Mater. Interfaces 3 (2011) 1827.
[7] A.M. Chaparro, B. Gallardo, M.A. Folgado, A.J. Martín, L. Daza, Catal. Today 143 (3—4) (2009) p.237.
[8] E. Passalacqua, F. Lufrano, G. Squadrito, A. Patti, L. Giorgi, Electrochim. Acta 46 (6) (2001) 799.
[9] M. Uchida, Y. Aoyama, N. Eda, A. Ohta, J. Electrochem. Soc. 142 (1995) 4143.
[10] J.M. Song, S.Y. Cha, W.M. Lee, J. Power Sources 94 (2001) 78.
[11] M. Aizawa, H. Gyoten, J. Electrochem. Soc. 160 (4) (2013) F417.
[12] L. Pu, J. Jiang, T. Yuan, J. Chai, H. Zhang, Z. Zou, X.-M. Li, H. Yang, Appl. Surf. Sci. 327 (2015) 205.
[13] T. Soboleva, X. Zhao, K. Malek, Z. Xie, T. Navessin, S. Holdcroft, Appl. Mater. Interfaces 2 (2) (2010) 375.
[14] K. Jayasayee, A. Zlotorowicz, D.P. Clos, Ø. Dahl, M.S. Thomassen, P.I. Dahl, S. Kjelstrup, ECS Trans. 6 (3) (2014) 321.
[15] Y.-H. Cho, J.W. Bae, O.-H. Kim, J.Y. Jho, N. Jung, K. Shin, H. Choi, H. Choe, Y.-H. Cho, Y.-E. Sung, J. Membr. Sci. 467 (2014) 36.
[16] M. Eikerling, A.S. Ioselevich, A.A. Kornyshev, Fuel Cells 4 (3) (2004) 131.
[17] J.H. Nam, M. Kaviany, Int. J. Heat Mass Transfer 46 (24) (2003) 4595.
[18] C. Lim, C.Y. Wang, Electrochim. Acta 49 (24) (2004) 4149.
[19] S. Chan, C.C. Wan, J. Power Sources 50 (1994) 261.
[20] S. Kjelstrup, M.-O. Coppens, J.G. Pharoah, P. Pfeifer, Energy Fuels 24 (9) (2010) 5097.
[21] E. Johannessen, S. Kjelstrup, Chem. Eng. Sci. 60 (2005) 1199.
[22] S. Kjelstrup, D. Bedeaux, E. Johannessen, J. Gross, Non-Equilibrium Thermodynamics for Engineers, World Scientific, Singapore, 2010.
[23] M.S. Saha, D.K. Paul, B.A. Peppley, K. Karan, Electrochem. Commun. 12 (2010) 410.
[24] G. Wang, M.-O. Coppens, Ind. Eng. Chem. Res. 47 (2008) 3847.
[25] J. Marquis, M.-O. Coppens, Chem. Eng. Sci. 102 (2013) 151.
[26] S. Martin, P.L. Garcia-Ybarra, J.L. Castillo, Int. J. Hydrogen Energy 35 (2010) 10446.
[27] D. Ebbing, S.D. Gammon, General Chemistry, tenth ed., Brooks/Cole, 2011, p. 465.
[28] D.W. Richerson, Modern Ceramic Engineering. Properties, Processing and Use in Design, third ed., 2006, p. 184. Taylor & Francis Group.
[29] T.E. Springer, T.A. Zawodzinski Jr., S. Gottesfeld, J. Electrochem. Soc. 138 (1991) 2334.
[30] T.L. Pugh, W. Heller, J. Colloid Sci. 12 (1957) 173.